PROC. INST. ACOUSTICS VOL 7 PT 3 1985

REFLECTIVITY PRODUCED BY A TARGET (HOLLOW SPHERE) BURIED IN A SAND BOTTOM

R. Carbó-Fité and C. Ranz-Guerra

Hydroacoustics Lab. Instituto de Acústica. c/ Serrano 144
28006 Madrid. Spain.

INTRODUCTION

There exist a great number of papers dealing with the target strength of targets of various shapes at different experimental circumstances. The analysis of the target is normally made in the time space. This paper presents some experimental results together with their corresponding computer models, refering to a target buried in a sand bottom.

The target we refer to consisted in an air filled hollow sphere. The sandy bottom was made covering with sand the bottom of an experimental tank (7.5 m x 4.5 m x 4.5 m) of the Hydroacoustic Laboratory at the Instituto de Acústica, in Madrid. The sand covered surface was 6 m x 4.5 m and the depth of the layer was 0.5 m about.

Two different methods were followed in investigating first the presence (or not) of the buried sphere, and scondly the evaluation of its most representative characteristics.

In the first of the two methods, the emitter-receiver system swept acoustically, according to a previously fixed program, a wide zone of the tank bottom, taking samples of the echo received from it (the pulse length and the pulse repetition frequency were chosen such that all the reflection from walls and other unwanted reflectors were avoided); the echo was filtered through time windows of 0.1 and 0.2 ms, the signal was rectified afterwards and the DC value (proportional to the RMS amplitude) recorded; the rectified value was, after filtering, compared (divided) with the DC value corresponding to the direc pulse emitted, also filtered.

In the second method the signal once cut from the whole ensemble of received signals, was analysed taking special look at: its shape; its structure in the frequency space and reflectivity. The magnitudes characterizing the target: depth of burial and dimensions were extracted from the experimental results.

In the analysis of this experience several hypothesis were set: I) The sand bottom surface is perfectly flat and parallel to the plane in which the emiter-receiver system mouves; II) The sand bottom is isotropic and homogeneous; III) Both, emitter and receiver are omnidirectional; IV) The sand bottom is considered a fluid medium in which does not exist transversal perturbations. The hypothesis I, III and IV are easily assumed in the experience. The III) because the isonified angles of interest are very small, and always remain within the emitter-receiver beamwidth; the IV) can be accepted as such considering that the transversal propagation velocity c_T is very much lower than the longitudinal c_e; the I) is easily accepted by the experimental set-up itself. The hypothesis II is the most difficult to avoid because it was not easy to built an artificial sand bottom with homogeneous structure mainly due to the presence of micro-bubbles of air that were not possible to extract completelly even after inssuflacting high pressure water from the lower layer of the bottom. On the other hand other factors were taken into consideration: A) the sand absorption $|1|$; B) the dependence of the water sand transmission coefficient with the angle of incidence

C) the sound speed in the sand; D) the sphere diameter; E) the target strength of the sphere, measured in water; F) the echo structure, independently if the echo has reached or not the steady state (at the instant when the signal was recorded and processed).

In this second method the signal recorded was split in two main parts: the direct signal and the echo. Both were analysed: recorded, frequency analysed, and finally divided by the direct signal.

A second processing was carried out that consisted in introducing the actual direct emitted signal in memory of a computer. Several models were built to try to obtain a replica of the experimental results.

Figure 1 shows esquematically the experimental set up: The emitter radiated at 16 kHz, its bandwidth was 4000 Hz. The pulse length was varied between 0.1 m to 0.2 ms. The receiver was always located at 1 m from the emitter and its response was flat in the frequency range of interest.

THEORETICAL BASIS

The acoustic wave train radiated by the emitter "E" reaches the receiver "R" through three paths: a) directly, ER, b) by being reflected in the bottom surface following the path EQ + QR, and lastly c) by reflection in the target itself, EN + NO' + O'M + MR; Fig. 1. Calling H_o = ER, the distance emitter-receiver; H_1 = EQ, depth of the bottom measured from the emitter; H_2 = PO, depth at which the target is buried; r the sphere radius and D_o the distance from the emitter-receiver axis to the center of the sphere. By simple geometrical considerations together with the Snell's Law applied to the refraction sufered by the acoustic waves, it is easy to deduce the following two equations

$$D_o = r \operatorname{sen}\alpha + \left|H_2 + r(1 - \cos\alpha)\right| \operatorname{tg}(\alpha + \Theta) + (H_1 - H_o) \frac{\frac{C_1}{C_2} \operatorname{sen}(\alpha + \Theta)}{\sqrt{1 - \left|\frac{C_1}{C_2} \operatorname{sen}(\alpha + \Theta)\right|^2}}$$

and

$$D_o = r \operatorname{sen}\alpha + \left|H_2 + r(1 - \cos\alpha)\right| \operatorname{tg}(\alpha - \Theta) + H_1 \frac{\frac{C_1}{C_2} \operatorname{sen}(\alpha - \Theta)}{\sqrt{1 - \left|\frac{C_1}{C_2} \operatorname{sen}(\alpha - \Theta)\right|^2}}$$

where C_1 and C_2 are the sound propagation velocity in water and in sand. From the above system, both angles: α and Θ, are deduced; they will allow to get the acoustic path of the wave train reflected in the target, that in the sand is

$$H_3 = NO' + O'M = \left|H_2 + r\ (1 - \cos\alpha)\right| \left(\frac{1}{\cos(\alpha + \Theta)} + \frac{1}{\cos(\alpha - \Theta)} \right)$$

and in the water

$$H_4 = \frac{H_1}{\sqrt{1 - \left|\frac{C_1}{C_2} \operatorname{sen}(\alpha - \Theta)\right|^2}} + \frac{H_1 - H_o}{\sqrt{1 - \left|\frac{C_1}{C_2} \operatorname{sen}(\alpha + \Theta)\right|^2}}$$

At the receiver the wave trains will arrive with a time delay that is a function

of the corresponding path as well as of the media. In such cases the delays would be

a) "Direct" path, $\tau_1 = H_o/C_1$

b) Bottom reflected path, $\tau_2 = (H_1 + (H_1 - H_o))/C_1$

c) Target reflected path, $\tau_3 = \frac{H_3}{C_2} + \frac{H_4}{C_1}$

It is as well necessary to take into account the energy losses:

a) "Direct" path: Divergence losses $A_1 = \frac{A_o}{H_o}$

b) Bottom refracted path: Divergence losses and by reflection in the bottom

$$A_2 = \frac{A_o}{(2\,H_1 - H_o)} \cdot \frac{\rho_2\,C_2 - \rho_1\,C_1}{\rho_2\,C_2 + \rho_1\,C_1}$$

where ρ_1 and ρ_2 are the water and sand densities.

c) Sphere reflected path: Divergence losses, by oblique incidence transmission (between angles $\alpha+\Theta$ and $\alpha-\Theta$, water-sand path and sand-water path), by sand absorption and by reflection in the target.

$$A_3 = \frac{A_o}{H_3 + H_4}\; T_{12} \cdot T_{21}\; e^{-\mu H_3} \cdot \sigma_{sph}$$

where

$$T_{12} = \frac{\rho_1}{\rho_2} \; \frac{\dfrac{2\,\rho_1\,C_1}{\sqrt{1 - \left[\dfrac{C_1}{C_2}\,\text{sen}\,(\alpha-\Theta)\right]^2}}}{\dfrac{\rho_2\,C_2}{\cos(\alpha-\Theta)} + \dfrac{\rho_1\,C_1}{\sqrt{1 - \left[\dfrac{C_1}{C_2}\,\text{sen}\,(\alpha-\Theta)\right]^2}}}$$

and

$$T_{21} = \frac{\rho_2}{\rho_1} \; \frac{\dfrac{2\,\rho_2\,C_2}{\cos\,(\alpha+\Theta)}}{\dfrac{\rho_2\,C_2}{\cos(\alpha+\Theta)} + \dfrac{\rho_1\,C_1}{\sqrt{1 - \left[\dfrac{C_1}{C_2}\,\text{sen}\,(\alpha+\Theta)\right]^2}}}$$

σ_{sph} is the target reflection coefficient |2|. μ is the sand absorption.

From the above relationship if the radiated signal is of the form X(t), the received signal will be

$$Y(t) = A_1\,X(t - \tau_1) + A_2\,X\,(t - \tau_2) + A_3\,X\,(t - \tau_3)$$

Being X(t) a short duration pulse (T) in the way that the distance H_1 is greater

than H_o plus the length C_1T, it is possible to separate the direct pulse

$A_1\ X(t - \tau_1)$

from the reflected

$A_2\ X(t - \tau_2) + A_3\ X(t - \tau_3)$

considering both pulses in the origin of time; so

$X_{Direct} = A_1\ X(t),\quad X_{Reflected} = A_2\ X(t) + A_3\ X(t - \tau)$

where $\tau = \tau_3 - \tau_2$

The next step is to get the quotient of the power spectral densities of both signals. First we calculate their FFT

$x_o(\omega) = A_1 x(\omega),\quad x_R(\omega) = A_2 x(\omega) + A_3 x(\omega) e^{-j\omega\tau}$

or $x_R = x(\omega)\ (A_2 + A_3\ e^{-j\omega\tau})$

and then the respective spectral densities

$\gamma_D(\omega) = x_D(\omega) . x_D(\omega)^*$

$\gamma_R(\omega) = \gamma_D(\omega)\ (A_2 + A_3\ e^{-j\omega\tau})\ (A_2 + A_3\ e^{j\omega\tau})/A_1^2$

so the final ratio is

$$\frac{\gamma_R(\omega)}{\gamma_D(\omega)} = \frac{A_2^2}{A_1^2} + \frac{A_3^2}{A_1^2} + \frac{2A_2A_3}{A_1^2}\ \cos\ \omega\tau$$

that will vary with the frequency as a cosine function between the maximum value, $\frac{A_2 + A_3}{A_1}$ for frequencies

$f_n = \frac{n}{\tau}$, (n = 1, 2, 3, ...) and a minimum $(A_2 - A_3)/A_1$

for frequencies $f_n = \frac{2n + 1}{2\tau}$

The separation among two consecutive maxima or minima is $\Delta f = 1/\tau$ and the difference between both maximum and minimum is $2A_3/A_1$ and their sum is $2A_2/A_1$.

RESULTS

Fig. 2 shows the reflectivity map obtained with the Method M1. The results are not very conclusive mainly because its difficulty in getting them, when it is necessary to take measurements at very short distances. The higher level of the reflectivity shows the presence of an important target that coincides with the location of the hollow sphere.

Let us examine some of the results of Method 2 Fig. 3 shows a sample of the direct signal and the echo analised. Fig. 4 shows the spectral level and its variation with the straight distance D_o to the vertical at which the target is buried , each curve corresponds to a variation ΔD_o = 0.025 m. Fig. 5 shows the results got in a computer in which the direct signal was input together with the target strength, the distance D_o, the depth at which the target is located, the

diameter of the target, as well as those characteristics of the media: water and sand, etc. Each group corresponds to a buried sphere at increasing depths from 0.05 m to 0.25 m. The change in the D_o coordinate, for each one of the curves, is ΔD_o = 0.05 m. The experimental results coincide with those in which the target is buried at a depth of 0.2 m, as it should be. Fig. 6-a) presents some of the results when, in the computer model, the experimental target strength was introduced (this datum was obtained with an sphere identical to the one buried, with only water around it [3]); in this figure the data refers to a target buried at 0.15 m and 0.20 m. Fig. 6-b) shows the variation of reflectivity in the same frequency range. The experimental reflectivity is presented in Fig. 7. By comparison of this result with that of figure 6, the periodic variation of the reflectivity is clear as well as the shift to lower frequencies when D_o increases. The irregularities that appear in the experimental results could be caused by the inhomogeneities of the artificial bottom studied that it was not considered in the computer models.

CONCLUSIONS

All the results seem to demonstrate that an analysis of the spectral level of the echo from the whole sand+sphere column can give an indication of the situation of the target as well as its characteristics. These data together with the reflectivity could be enough to give an account of the unknown target.

REFERENCES

[1] E.L. Hamilton, "Oceanographic models of the sea floor", Physics of Sound in marine Sciences, L. Hampton, Ed. Plenum Press, London, pp 181-221, (1974).

[2] C.B. Officer, "Introduction to the Theory of Sound Transmission" McGraw-Hill Book Co. London, pp 185-248, (1958)

[3] R.W.G. Harlett, "Acoustic Echoes from targets under water", Underwater Acoustics. R.W.B. Stephens. Ed. Wiley-Interscience. London, pp 129-197 (1970).

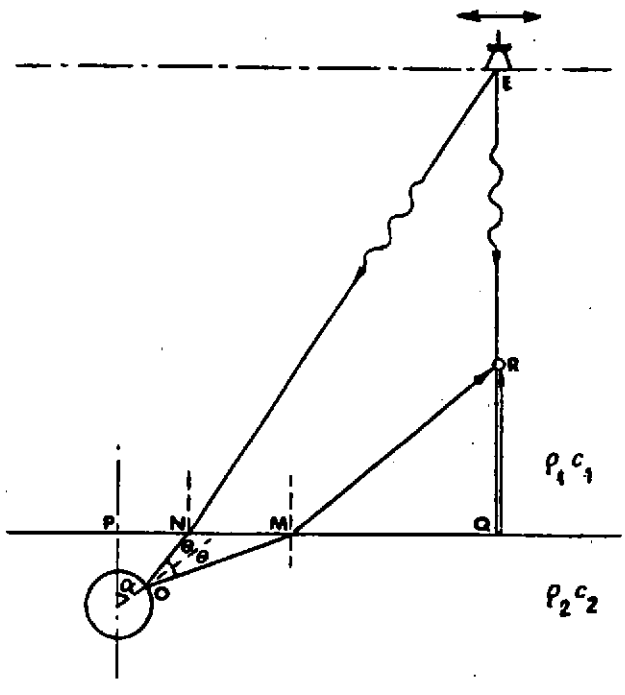

Fig. 1. Experimental set-up

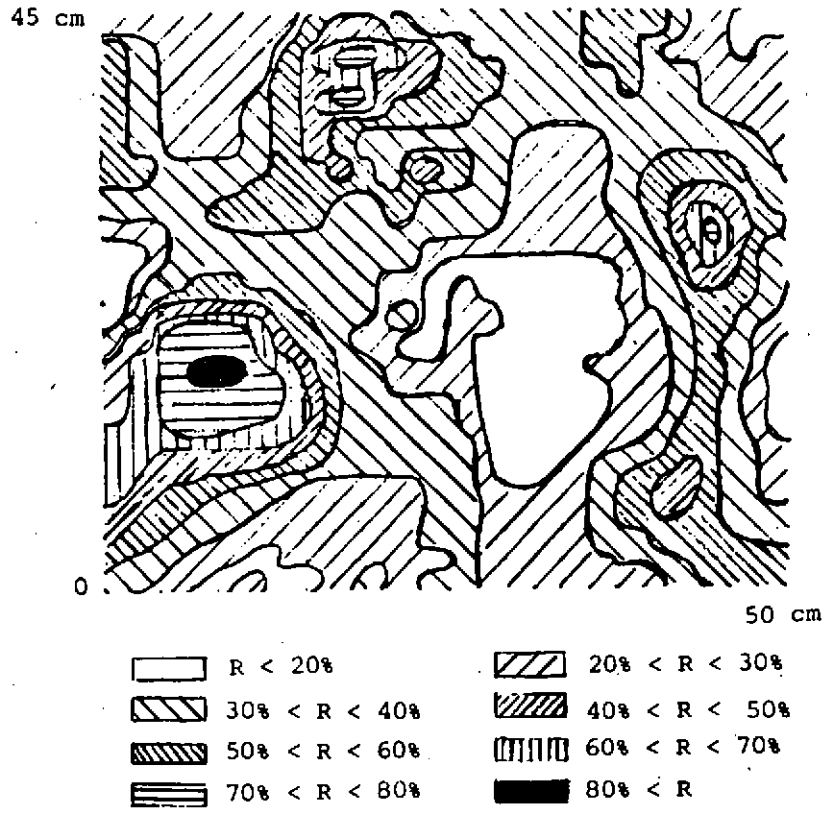

Fig. 2. Experimental Reflectivity Map

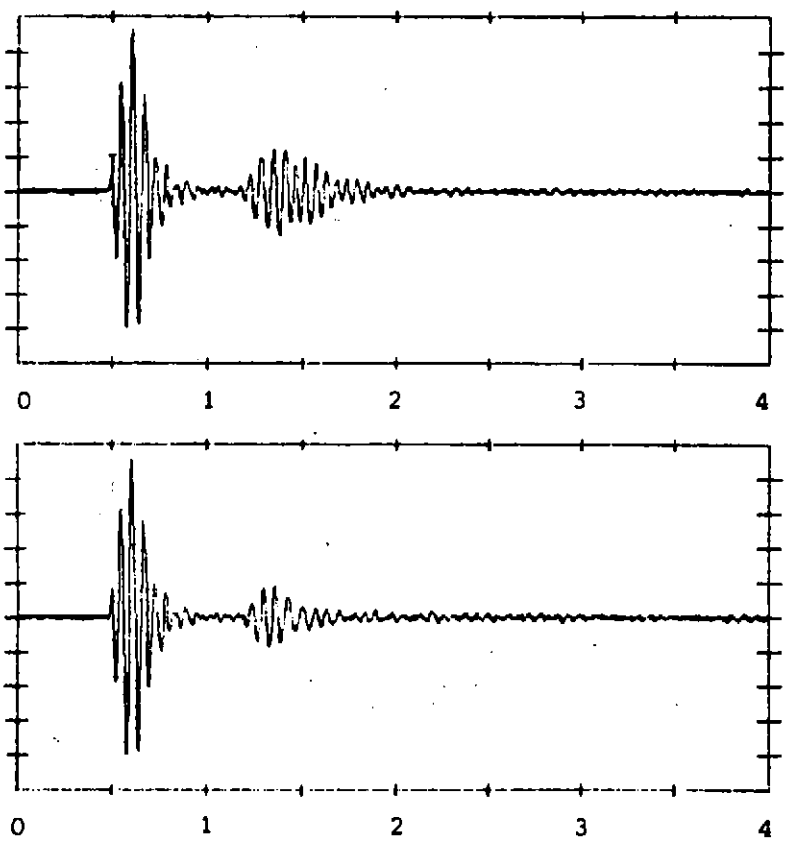

Fig. 3. Direct signal and echo-signal

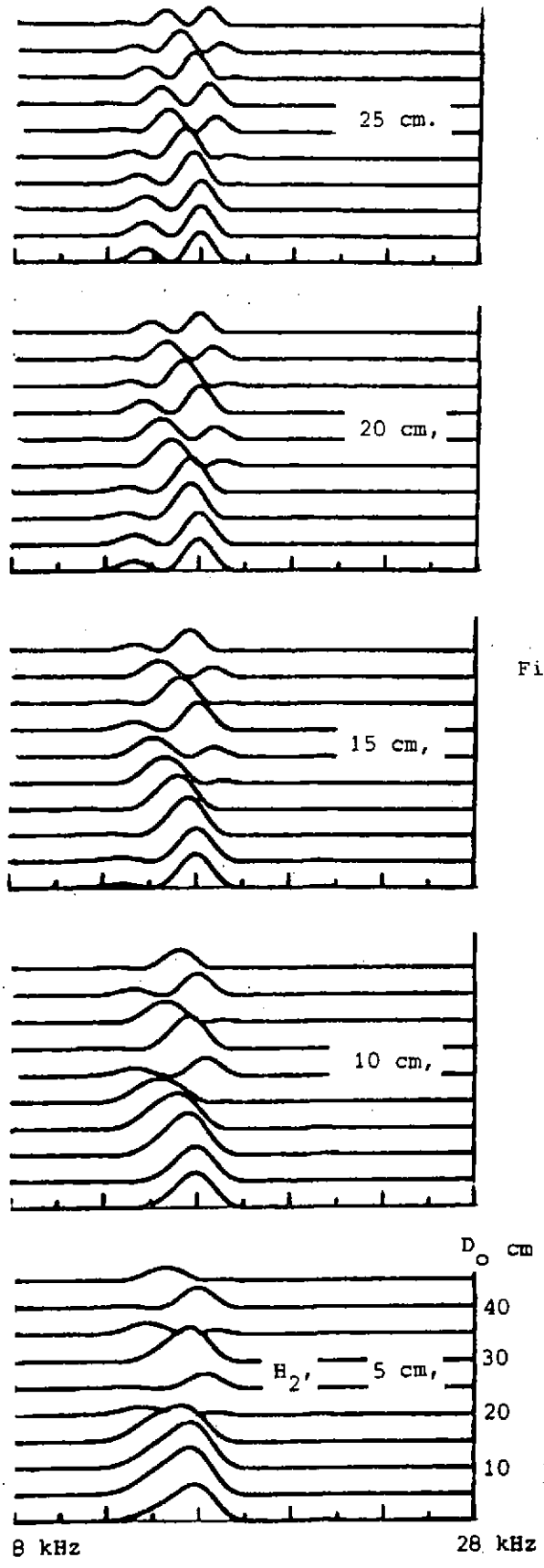

Fig. 5. Computer simulation with actual data input. Each group represents a different burial depth H_2; The increasing D_o distance is the parameter of each curve. The horizontal axis is frequency and the ordinate the spectral density.

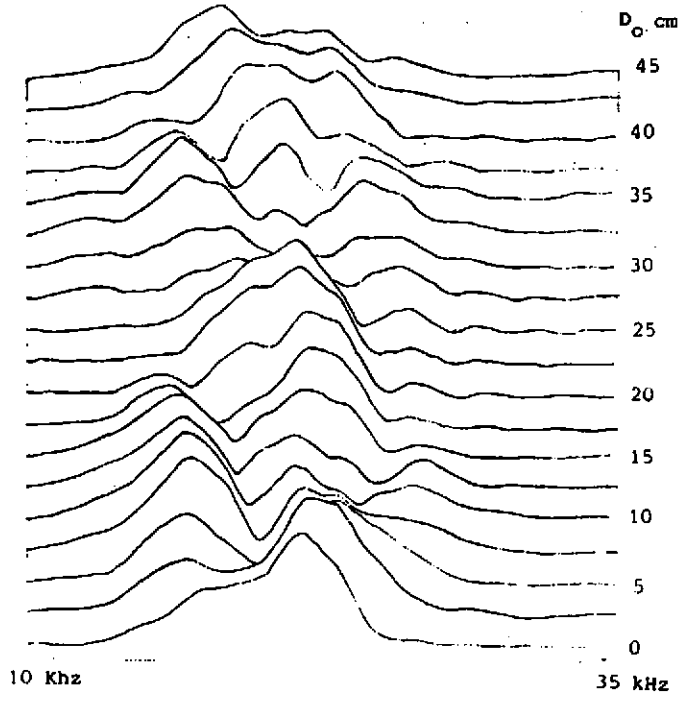

Fig. 4. Spectral density (experimental) of the echo

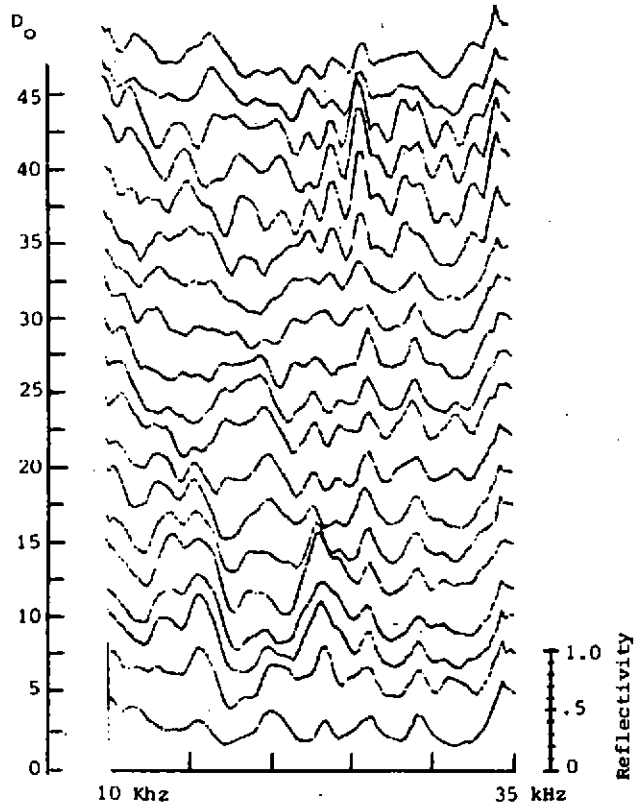

Fig. 7. Experimental reflectivity Horizontal axis: frequency; vertical axis. spectral density. Each curve parameter represents a DØ distance varying from DØ=0 to DØ=.45m in increments of 0.025m.

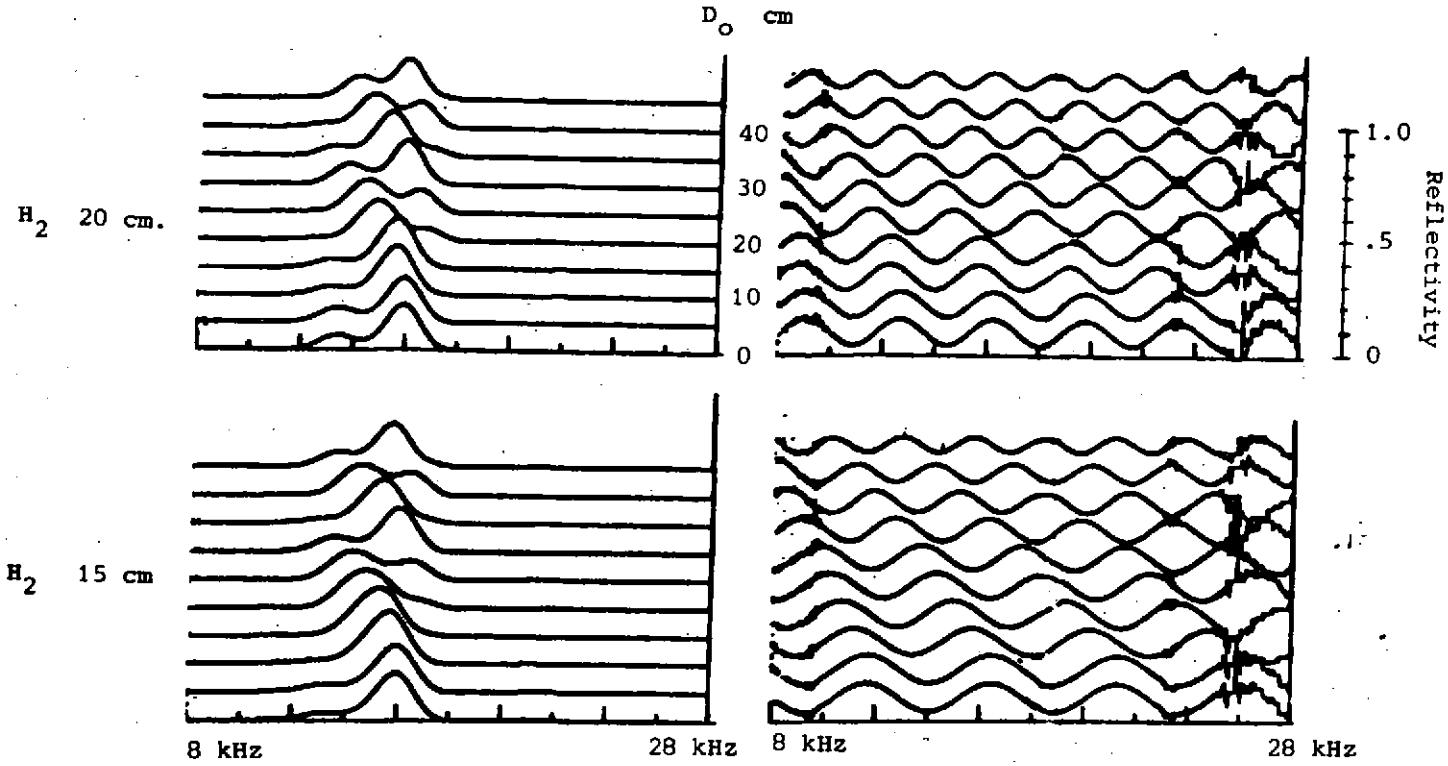

Fig. 6. Computer simulation with actual target strength
a) Horizontal axis: frequency; vertical axis: spectral density
b) Horizontal axis: frequency; vertical axis: reflectivity.